Available online at www.sciencedirect.com
ScienceDirect
Catalysis Today 136 (2008) 206–213
CATALYSIS TODAY
www.elsevier.com/locate/cattod

Catalytic partial oxidation of *n*-tetradecane using pyrochlores: Effect of Rh and Sr substitution

Daniel J. Haynes [a,b,c,*], David A. Berry [a,1], Dushyant Shekhawat [a,2], James J. Spivey [c,3]

[a] *U.S. Department of Energy, National Energy Technology Laboratory, 3610 Collins Ferry Road, Morgantown, WV 26507, USA*
[b] *Parsons, P.O. Box 618, South Park, PA 15129*
[c] *Louisiana State University, Department of Chemical Engineering, 110 South Stadium Drive, Baton Rouge, LA 70803, USA*

Abstract

The catalytic partial oxidation (CPOX) of transportation fuels into synthesis gas (H_2 + CO) for fuel cells is complicated by the large quantities of aromatics and sulfur-containing compounds commonly found in these fuels. Traditional supported metal catalysts are easily poisoned by these species which adsorb strongly onto the electron-rich metal clusters. The use of noble metal and/or oxide based catalyst systems may offer higher activity and stability, but only if the metal can be bound into a thermally stable structure. To that end, Rh metal was substituted into the structure of a lanthanum zirconate (LZ) pyrochlore to give $La_2Rh_yZr_{(2-y)}O_{(7-\xi,)}$ (LRZ) to produce a strongly bound, well-dispersed metal which is active for CPOX. A second catalyst was prepared in which Sr was substituted for a portion of La in the LRZ structure, producing $La_{(2-x)}Sr_xRh_yZr_{(2-y)}O_{(7-\xi)}$ (LSRZ). Each of these pyrochlore catalysts, including the unsubstituted LZ, were characterized and screened for activity in the CPOX of *n*-tetradecane (TD), which is a surrogate for linear paraffins typical of diesel fuel. Results were compared to a commercial Rh/γ-Al_2O_3 catalyst.

X-ray diffraction patterns of both the LZ and LRZ showed that each had the cubic unit-cell pyrochlore structure. However, substitution of Sr resulted in a binary perovskite-pyrochlore phase with a defect $SrZrO_3$ phase. Hydrogen pulse chemisorption and temperature programmed reduction studies confirmed that Rh metal was substituted into the structure of the LRZ and LSRZ, and was reducible. Activity screening with the CPOX of TD showed that the Rh substituted in both LRZ and LSRZ is able to retain activity-producing essentially equilibrium synthesis gas yields, as was the Rh/γ-Al_2O_3. Temperature programmed oxidation experiments performed after the CPOX of TD demonstrated that the amount of carbon was quantitatively similar for each catalyst (roughly 0.3 $g_{carbon}/g_{catalyst}$ after each run), with the exception of LSRZ, which had significantly less carbon (0.17 $g_{carbon}/g_{catalyst}$). It is speculated that improved oxygen ion mobility in the LSRZ material, which resulted from Sr substitution, was responsible for the reduction in carbon formation on the surface.
Published by Elsevier B.V.

Keywords: Partial oxidation; Rhodium; Logistic fuel reforming; Diesel; Pyrochlore; Catalyst deactivation

1. Introduction

Fuel cells provide a clean, efficient alternative to conventional energy conversion processes. However, widespread use of fuel cells requires a production and distribution network for the hydrogen-rich gas stream that these units require. Although such a network does not yet exist [1–3], widely available logistic fuels, like diesel, can be readily reformed into a hydrogen-rich gas that can be used directly in fuel cells [4,5].

Solid oxide fuel cells (SOFCs) operate at temperatures sufficiently high that a gas stream consisting of both H_2 and CO can be used. This allows the use of reformate from hydrocarbon fuels to be used directly in SOFCs without CO removal steps. SOFCs have been targeted by the U.S. Department of Energy and others for near term commercialization [6–11], and the development of catalysts for reforming of diesel (and other liquid fuels) is essential for these fuel cells to become widely used.

Three main catalytic reforming reactions can be used to convert liquid fuels into synthesis gas (H_2 + CO) for fuel cells: steam reforming (SR), catalytic partial oxidation (CPOX), and

* Corresponding author. Present address: Parsons, P.O. Box 618, South Park, PA 15129, USA. Tel.: +1 304 285 1355; fax: +1 304 285 0903.
E-mail addresses: Daniel.Haynes@pp.netl.doe.gov (D.J. Haynes), David.Berry@netl.doe.gov (D.A. Berry), Dushyant.Shekhawat@netl.doe.gov (D. Shekhawat), jjspivey@lsu.edu (J.J. Spivey).
[1] Tel.: +1 304 285 4430.
[2] Tel.: +1 304 285 4634.
[3] Tel.: +1 225 578 3690.

0920-5861/$ – see front matter. Published by Elsevier B.V.
doi:10.1016/j.cattod.2008.02.012

autothermal reforming (ATR).

$$\text{SR}: \quad C_nH_m + H_2O \rightarrow H_2 + CO_x \qquad \Delta H > 0$$

$$\text{CPOX}: \quad C_nH_m + O_2 \rightarrow H_2 + CO_x \qquad \Delta H < 0$$

$$\text{ATR}: \quad C_nH_m + O_2 + H_2O \rightarrow H_2 + CO_x \qquad \Delta H \sim 0$$

CPOX is considered a practical reforming method to be used for remote and logistical purposes [1,12]. Because the reaction is exothermic, the reformer does not need to be as optimized for heat transfer, like SR and ATR, and can be lighter and more compact [13]. The high reaction temperatures associated with CPOX minimize carbon and sulfur poisoning [5], improve response to transients in the feed flow rate [14], and allow for rapid start-up. In addition, no water storage or delivery system is required, which makes the reforming system less complex and reduces its cost [14,15].

As advances in SOFC design bring the technology closer to a commercial product, a long-life CPOX reformer is required. An analysis of the CPOX reformer shows that it should be capable of 5000 h of continuous operation before it can be used for practical applications [16]. Recent literature shows that the CPOX of higher hydrocarbons is capable of producing high synthesis gas yields with high conversion of fuel with an appropriate catalyst [17–25]. However, long-term CPOX reaction experiments are hindered by the deactivation of the catalyst by the aromatic and sulfur compounds commonly found in diesel fuel [5,21].

CPOX catalysts typically consist of Ni [14] or Group-VIII noble metals [17,18,23,26,27] incorporated onto various high surface area oxide substrates such as γ-Al_2O_3, SiO_2, and more recently, mixed metal oxides [21,28]. From the literature [19,25,29,30], Rh has been identified as the superior metal for CPOX due to its high selectivity to H_2 and CO. This behavior is believed to be directly related to the high bond strength of Rh metal with surface oxygen, which prevents the undesirable reaction between surface oxygen and dissociated hydrogen atoms on the surface to form hydroxyl radicals, and eventually water [25]. Also, Rh has shown a high resistance to carbon formation compared to other metals [18,21,31].

However, carbon formation and deactivation by sulfur are key challenges for CPOX catalysts. It has been shown that catalyst poisoning by sulfur and/or carbon is a structure sensitive reaction [22,32]. Specifically, the deactivation mechanism by carbon and sulfur is influenced by the cluster size of the active metal. For example, larger metal clusters have a much stronger interaction with carbon and sulfur, than smaller, well-dispersed metal particles [32–34]. This problem becomes worse at the high reforming temperatures of CPOX, because conventional supported metals tend to sinter and agglomerate into even larger particles.

The development of a catalyst with spatially distributed active metal components in a structure that can tolerate the high temperatures of CPOX may provide a more durable catalyst compared to simple supported metal clusters. Dispersing the metal throughout the structure may avoid the formation of larger metal clusters at the surface that are favorable sites for sulfur poisoning and carbon deposition, and thus may make the catalyst less susceptible to deactivation. Mixed metal oxides have become increasingly popular because of the ability to substitute different metals into their structure and maintain catalytic activity [22,35,36]. For example, Gardner et al. [22] demonstrated the ability to effectively incorporate Ni into the hexaaluminate structure $ANi_{0.4}Al_{11.6}O_{19-\delta}$ (A = La, Sr, and Ba) and successfully partially oxidize *n*-tetradecane with reduced carbon formation. Liu and Krumpelt [35] have shown that the incorporation of Ru into a perovskite type structure ($LaCr_{0.95}Ru_{0.05}O_3$) is catalytically active for the ATR of *n*-dodecane while exhibiting sulfur tolerance.

Yet, the substitution is not exclusively limited to transition metals. To complement the catalytic activity, additional, lower valence elements (typically rare earth metals) can be substituted into the structure to create oxygen vacancies which increase oxygen ion mobility in the bulk material [35,37,38]. Oxygen mobility has been identified as a mechanism that can reduce carbon accumulation on the surface in reforming reactions. Erri et al. [37] reported that the addition of Ce to a Ni-containing perovskite ($La_{0.6}Ce_{0.4}Fe_{(1-x)}Ni_xO_3$) greatly reduces carbon formation in ATR of JP-8 military fuel. The defects cause oxygen anions to become more weakly bound in the crystal lattice, and these anions can then oxidize adsorbed carbon and its precursors.

Another class of mixed oxides, known as pyrochlores, shows potential to incorporate noble metals and other elements to form a catalyst with reduced carbon forming properties and high activities. A pyrochlore is a derivative of the fluorite structure. It is composed of 1/2 trivalent cations and 1/2 tetravalent cations in a cubic unit cell structure, shown in Fig. 1, with the general stoichiometry $A_2B_2O_7$ [38]. The A-site is usually a large cation (typically rare earth elements) and is coordinated with eight oxygen anions. The B-site cation has a smaller radius (usually transition metal) and is coordinated with six oxygen atoms. In order to form a stable pyrochlore, A and B cations must have an ionic radius ratio between 1.4 and 1.8 [39].

In choosing an appropriate material for CPOX, the pyrochlore must maintain chemical and thermal stability at

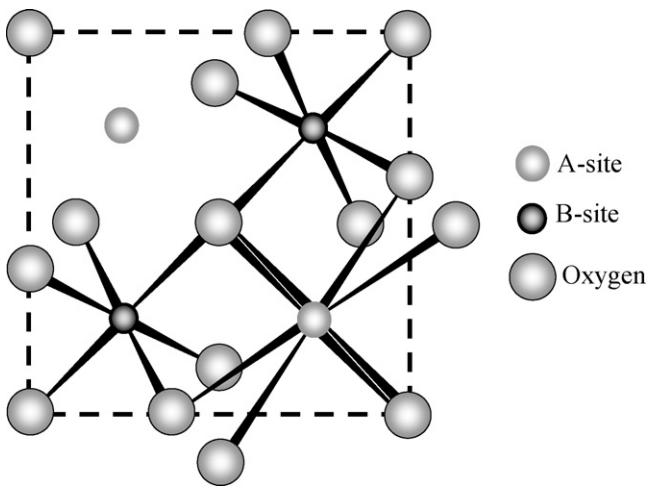

Fig. 1. General structure of $A_2B_2O_7$ pyrochlore. Figure adapted from [39].

reaction conditions. As a catalyst for CPOX, the lanthanum zirconate, $La_2Zr_2O_7$ (LZ) pyrochlore is of considerable interest. Although we are not aware of any studies of this material for reforming purposes, it has shown remarkable physical properties (e.g., thermal and chemical stability) that suggest it is an attractive option as a CPOX catalyst. The material is currently being investigated as an alternative to yttrium stabilized zirconia (YSZ) as a thermal barrier coating for turbine engines because it has a high melting point and chemical stability [40–43]. It also has shown the mechanical strength needed to accommodate the substitution of metals that improve oxygen ion conductivity [42].

However, before deactivation studies can be performed, it is necessary to understand the physical properties of the pyrochlore catalysts and to ensure they are active catalysts for CPOX. Thus, the purpose of this study is to evaluate a $La_2Zr_2O_7$ pyrochlore substituted with (a) Rh only, and (b) Rh + Sr for the CPOX reforming reaction. The catalysts are characterized to verify whether the Rh metal can be substituted into the structure and also to correlate the reforming activity with the physical and chemical properties of the substituted material. Finally, each catalyst is tested for activity by the CPOX of model compound *n*-tetradecane (TD), which is intended to be a surrogate for the linear paraffins typical of diesel fuel. Paraffins are also the most reactive compounds in logistic fuel mixtures and they make-up the largest portion of the fuels, roughly 40 wt% [44]. A temperature programmed oxidation (TPO) is performed after the activity study to analyze the formation of carbon on each catalyst. The results are compared to a conventional supported 0.5 wt% $Rh/\gamma\text{-}Al_2O_3$ catalyst to investigate the effects of substitution on catalytic properties of the Rh metal.

2. Experimental

2.1. Catalyst synthesis

The pyrochlore catalysts shown in Table 1 were prepared using a variation of the Pechini method [45–48], which produces highly uniform non-substituted and substituted catalyst crystals. Metal nitrates $La(NO_3)_3{\cdot}6H_2O$ (GFS Chemicals), $ZrO(NO_3)_2{\cdot}nH_2O$*, $Rh(NO_3)_3{\cdot}2H_2O$*, and $Sr(NO_3)_2$* (*Alfa Aesar) were used as metal precursors. The nitrates salts were dissolved separately in de-ionized water, and then combined with a citric acid (CA) solution in a 1:1 molar ratio of CA:metal. The solution was then heated to 75 °C while being stirred to ensure complete metal complexation. Once at 75 °C, a 40:60 molar ratio of ethylene glycol (EG) to CA was added the solution. The solution was left stirring on the hot plate until most of the water had evaporated and a transparent, viscous gel remained. At this point, the stir bar was removed from the beaker, and the gel was left on the hot plate (at 75 °C) to promote the polyesterification reaction between EG and CA and ultimately formed the organic polymeric network [49]. During this time, the gel began frothing and bubbling violently while large plumes of NO_x were emitted due to the decomposition of the nitrate precursors. The foam-like mass that remained was then placed in an oven at 110 °C to dry overnight. Following drying, the organic precursors were oxidized by calcination at 900 °C for 5 h to form the catalyst powders. The $Rh/\gamma\text{-}Al_2O_3$ (0.5 wt% Rh on 3 mm alumina pellets) catalyst was obtained commercially from Alfa Aesar (Stock # 42507).

2.2. Catalyst characterization

2.2.1. X-ray diffraction

Phase analysis of powder samples was examined using a PanAnalytical X'pert Pro X-ray diffraction system (model number PW 3040 Pro). The device consisted of a ceramic diffraction X-ray tube containing Cu Kα radiation at a wave length of Kα 1.54184 Å. Power requirements during operation were 45 kV and 40 mA. The divergence slit angle for the incident X-ray beam was set to 0.5° and the anti-scatter slit was 0.20°. The receiving slit of the diffracted beam was 2°. PDF-2, Release 2004 was used as the pattern identification database.

2.2.2. Temperature programmed reduction and H_2 pulse chemisorption

Temperature programmed reduction (TPR) and H_2 pulse chemisorption analyses were conducted with a Micromeritics Autochem 2910 unit. Before the start of the TPR, the catalyst was oxidized at 900 °C for 0.5 h under a 2% O_2/He mixture to burn off any impurities or residual material that may have remained on the surface from the synthesis. After the sample had cooled, it was ramped from 100 to 950 °C by 5 °C/min under the 5% H_2/Ar mixture and held at 950 °C for 30 min.

The amount of accessible Rh metal was determined by H_2 pulse chemisorption. Before chemisorption experiments, the catalyst was reduced under H_2, then purged under argon and cooled to 50 °C to begin chemisorption. At 50 °C, the catalyst was dosed with 0.5377 scc 5% H_2/Ar for 2 min. The dosing process was repeated until the metal surface was saturated with dissociated hydrogen. For H_2 dispersion, a 1:2 stoichiometric ratio of H_2:metal was used [50,51].

Table 1
Composition and Rh content of pyrochlore catalysts[a]

	$La_2Zr_2O_7$ (LZ)	$La_2Rh_{0.11}Zr_{1.89}O_{7-y}$ (LRZ)	$La_{1.5}Sr_{0.5}Rh_{0.10}Zr_{1.90}O_{7-y}$ (LSRZ)
Oxygen adjustment (y)	0	0.055	0.30
Rh content (wt%)	0	2.0	2.0

[a] Based on amounts of metals used in the preparation process.

2.3. CPOX activity measurements

2.3.1. Reactor setup

The reactor configuration used for the catalyst activity screening as well as its detailed description is documented elsewhere [21]. In short, catalyst testing took place in a fixed-bed continuous-flow reactor (Autoclave Engineers, Model no. BTRS Jr). The catalyst was placed in an 8 mm i.d. tubular reactor and diluted with quartz sand (5 g silica per 1 g catalyst) of the same particle size as the catalyst, to minimize temperature gradients and channeling throughout the bed. Heat was supplied via a split-tube furnace, which encapsulated the tubular reactor. Bed temperature was measured by an axially centered thermocouple and was controlled by a programmable controller. External heating was required to ensure a uniform temperature distribution throughout the catalyst bed. Although the CPOX reaction is highly exothermic, the reactant flow rates were too low for the reaction to sustain itself because of the significant heat losses caused by the systems size.

2.3.2. CPOX studies

n-Tetradecane (TD) was the surrogate diesel fuel used in this study. The CPOX of pure TD for 5 h was performed to examine the catalyst activity and product selectivity. Experimental conditions are detailed below in Table 2. After CPOX experiments a temperature programmed oxidation (TPO) was performed to determine the amount of carbon deposited on the spent catalyst. The carbon was oxidized by passing a 5% mixture of O_2/N_2 over the catalyst while it was heated from 200 to 900 °C by 1 °C/min. The catalyst was left at 900 °C overnight and cooled to ambient in the morning.

2.3.3. Product analysis

The dry gas products: H_2, CO, CO_2, CH_4 and N_2 were analyzed continuously by means of an online Thermo Onix mass spectrometer (Model no. Prima δb, a 200 a.m.u. scanning magnetic sector). Larger hydrocarbon products were analyzed with an HP5890 gas chromatograph equipped with a flame ionization detector. Carbon balances for all experiments were 100 ± 10%.

The following Eqs. (4.1)–(4.3) were used in the analysis of the experimental data. The yield of each dry gas product, i.e. H_2, CO, CO_2, and CH_4 was calculated by Eq. (4.1).

$$\text{Yield of A}\,(\%) = \frac{\text{Moles of A produced} \times 100}{N \times \text{moles of TD fed to the reactor}} \tag{4.1}$$

where N is the number of moles of H_2 per mole of hydrocarbon for H_2 yields and is the number of moles of carbon in the hydrocarbon fuel for yields of carbon containing products.

Hydrocarbon (HC) yields were determined using Eq. (4.2).

$$\text{HC yield}\,(\%) = \frac{\text{Moles of HC produced} \times i \times 100}{N \times \text{moles of TD fed to the reactor}} \tag{4.2}$$

where i is the number of moles of carbon per mole of hydrocarbon in the product (i.e. i would be 2 for ethane) and N is the number of moles of carbon in the hydrocarbon fuel.

A carbon balance was determined by Eq. (4.3).

$$\text{Carbon balance}\,(\%) = \frac{(\text{CO} + \text{CO}_2 + \sum_i^{i=1-6} i\text{C}_i\text{H}_r) \times 100}{N \times \text{moles of TD fed to the reactor}} \tag{4.3}$$

where i is the number of moles of carbon per mole of hydrocarbon in the product (i.e. i would be 2 for ethane), N is the number of moles of carbon in the hydrocarbon fuel and r is the number of hydrogen atoms contained in the hydrocarbon product.

Table 2
Experimental conditions for CPOX experiments

Feed concentration	mmol/L	mol%
N_2	36.0	80.1
O_2	8.0	17.8
TD	0.95	2.1
O/C	1.2	
GHSV (scc $g_{catalyst}^{-1}$ h^{-1})	50,000	
Pre-heat (°C)	375	
Temperature (°C)	900	
Catalyst bed (mg)	480	
Pressure (MPa)	0.23	

3. Results/discussion

3.1. Characterization

3.1.1. X-ray diffraction

The X-ray diffraction (XRD) patterns for the pyrochlore catalysts after calcination are shown in Fig. 2. The XRD of LZ demonstrates a single-phase, cubic unit cell structure distinctive to the pyrochlore and resembles similar patterns seen in the literature [42,52]. The similar diffraction pattern for LRZ indicates the metal loading of Rh (2 wt%) is low enough that substituting for the B-site Zr^{4+} ions does not result in any peak shifts or phase changes in the bulk crystalline properties of the

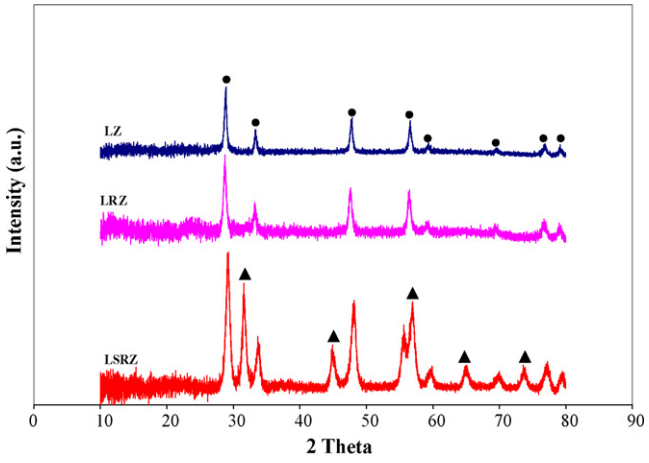

Fig. 2. XRD patterns illustrating the structural changes on LZ after substitution of Rh only, and Rh and Sr. (●) Peaks from $La_2Zr_2O_7$ pyrochlore; (▲) peaks from $SrZrO_3$ perovskite.

material. The substitution of the larger ionic radius Sr^{2+} (0.126 nm in 8-fold coordination) for the smaller La^{3+} (0.116 nm in 8-fold coordination) expands the lattice parameter of the pyrochlore structure [53,54]. This is evident in Fig. 2 as the pyrochlore peaks in LSRZ are shifted to slightly higher 2θ values compared to LZ. In spite of this, it appears only some of Sr was substituted into the structure, as a separate $SrZrO_3$ perovskite phase forms in addition to the pyrochlore. This is consistent with two studies involving Zr-pyrochlores [53,54]. In a study to determine the durability of $La_2Zr_2O_7$ pyrochlore to encapsulate simulated high-level nuclear waste products Ce and Sr, Hayakawa and Kamizono [53] found Sr to be only 2.5 mol% soluble in the structure, while excess Sr would lead to the formation of $SrZrO_3$. In a similar study Patwe and Tyagi [54] found that only 1.2 mol% Sr can be substituted into the structure of $Gd_2Zr_2O_7$ pyrochlore before the $SrZrO_3$ phase forms. Thus, with the amount of Sr used in this study, the LSRZ is likely a composite material with a contiguous mixture of Rh-doped $La_2Zr_2O_7$ and $SrZrO_3$. It should be noted that as there are two phases present, both phases may contribute to the observed catalytic activity. The extent of activity that can be attributed to each phase is unknown in this study, and will be subject of further research.

3.1.2. Temperature programmed reduction

TPR profiles for the catalysts used in this study are shown in Fig. 3. The reduction of Rh/γ-Al_2O_3 shows two peaks (136 °C and 260 °C). These can be attributed to the reduction of two different rhodium oxide species (RhO_x) [55–58], although the exact peak reduction temperatures observed here differ slightly from literature values [55,57], likely due to the extent of interaction between the rhodium and alumina support. Reduction of the LZ exhibits a single, broad peak at 527 °C. LRZ and LSRZ each show high temperature peaks similar to the LZ, at 549 °C and 540 °C, respectively. The peak is shifted to a slightly higher temperature, compared to LZ, probably as a result of the substitution of Rh and Sr into the LZ structure.

After Rh substitution, a distinct, low temperature peak (280 °C for LRZ and 274 °C for LSRZ) occurs. This peak appears to be qualitatively similar to the high temperature peak (260 °C) of the Rh/γ-Al_2O_3, only shifted to a slightly higher temperature, likely due to the interaction of Rh with surrounding elements in the pyrochlore structure. This is an indication that even though Rh is substituted throughout the structure, some Rh atoms are accessible at the surface and can be reduced. The two peaks are likely the result of the reduction of a small amount of partially coordinated surface Rh atoms to their metallic state. Fig. 3 also shows that the low-temperature reduction peak seen for the Rh/γ-Al_2O_3 (136 °C) is not present in either of the Rh-substituted pyrochlores. This shows that the Rh in the pyrochlores is present in a different, less easily reduced state in the Rh/γ-Al_2O_3.

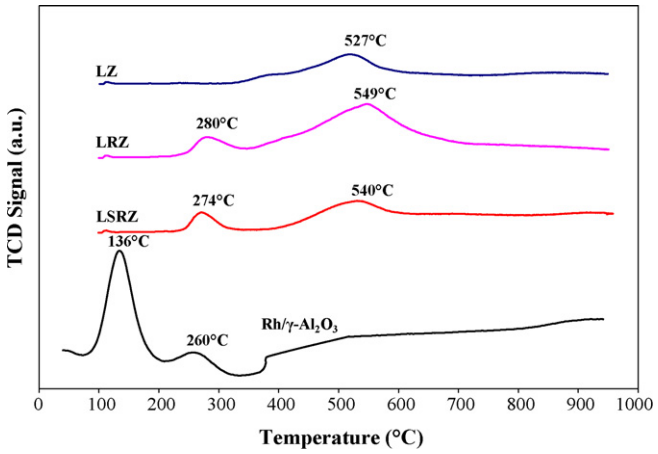

Fig. 3. TPR results illustrating the change in reduction properties of LZ after the addition of Rh only (LRZ), or Rh and Sr (LSRZ) and compared to Rh/γ-Al_2O_3.

3.1.3. H_2 pulse chemisorption

Table 3 shows that the amount of accessible Rh metal at the surface of the pyrochlores is less than that for the Rh/γ-Al_2O_3. Although low dispersion values for the LRZ and LSRZ might suggest that large Rh metal clusters may have formed on the surface, the lack of a low temperature reduction peak (136 °C) for Rh in the pyrochlores in Fig. 3 (which is seen for the Rh/γ-Al_2O_3), indicates that most of the metal is contained within the structure.

3.2. CPOX of TD-only

3.2.1. Thermodynamic equilibrium and blank reactor

The activity and selectivity of each catalyst was evaluated by the CPOX of TD for 5 h. However, before catalytic testing, thermodynamic equilibrium product yields were calculated at reaction conditions to serve as a reference to judge catalytic activity. Also, the CPOX of TD was performed in a blank reactor to provide a reference for the catalytic reactions. These results are presented in Table 4.

Equilibrium values were determined by a Gibbs free energy minimization calculation using HSC Chemistry software [59]. The calculations were made assuming a mixture of 2 mol% TD, 18 mol% O_2, and 80 mol% N_2 (O/C = 1.2), 0.23 MPa and 900 °C. The thermodynamic equilibrium values indicate that, at reaction conditions used in this study, equilibrium H_2 and CO yields are high, with a ratio of H_2/CO slightly <1, with no C_2–C_6 hydrocarbon formation.

Product yields from the CPOX of TD over inert quartz sand (Table 4) are similar to a blank that was run previously in this same system, under the same conditions, only at 850 °C [60]. It can be seen that a significant amount of the TD is converted to olefins and benzene (~23%), as well as lower hydrocarbons such as methane (~8%), which are not predicted by equilibrium. Ethylene is the main gas-phase reaction product

Table 3
Effective Rh content of each catalyst studied

Catalyst	%Accessible
Rh/γ-Al_2O_3 (0.51 wt% Rh)	72.6
LRZ (2 wt% Rh)	1.9
LSRZ (2 wt% Rh)	4.7

Table 4
Equilibrium and blank reactor (quartz sand) product yields, and carbon balance for the CPOX of TD at O/C = 1.2, P = 0.23 MPa, 900 °C and 50,000 scc $g_{catalyst}^{-1}$ h^{-1}

	Equilibrium[a]	Quartz sand (blank)
H_2 yield (%)	90.0	17.0
CO yield (%)	92.0	42.0
CO_2 yield (%)	8.5	17.0
CH_4 yield (%)	0.1	8.0
Ethane yield (%)	0.0	0.70
Ethylene yield (%)	0.0	16.30
Propylene yield (%)	0.0	1.5
C_4-ene yield (%)	0.0	1.0
Benzene yield (%)	0.0	3.90
Carbon balance (%)	100	90

[a] Equilibrium calculations were made using a Gibb's minimization technique in HSC Chemistry software. Calculations were made assuming a mixture of 2 mol% TD, 18 mol% O_2, and 80 mol% N_2.

that forms over the quartz, which is consistent with other results [30,61]. Although these hydrocarbons contain H_2, their formation cannot account for the difference in H_2 yields compared to equilibrium values. A mass balance for unconverted O_2 and H_2 atoms shows an H/O ratio of roughly 2.4 over the 5 h experiment, suggesting that water formation is occurring (water was not quantitatively analyzed here).

3.2.2. CPOX catalysts

Reforming results for Rh/γ-Al_2O_3 as well as those for the unsubstituted and substituted pyrochlores after the CPOX of TD for 5 h are shown in Table 5. Each catalyst exhibits steady reforming yields over the 5 h experiment, with all catalysts showing >95% conversion of TD to gaseous hydrocarbons products. The H_2, CO, CO_2 and CH_4 yields produced over the LSRZ are presented in Fig. 4 to illustrate the activity over this time period.

The H_2 and CO yields produced over Rh/γ-Al_2O_3 were close to equilibrium levels while olefin and benzene yields remained low, which indicates Rh is highly active for the CPOX of higher hydrocarbons. This activity is consistent with the results from Schmidt's group [17,23,24,27,62], who have reported high H_2 and CO selectivities (>70%) for the CPOX (O/C = 1.2) of *n*-decane [17,23] and *n*-hexadecane [17,62] over a Rh/γ-alumina coated onto an α-Al_2O_3 foam monolith.

In comparison to the Rh/γ-Al_2O_3, LZ is less selective towards synthesis gas, which is to be expected in the absence of a noble metal. The carbon balance shows all carbon is accounted for within experimental error, but the LZ pyrochlore

Table 5
Product yields and carbon balance for Rh/γ-Al_2O_3 and pyrochlores after 5 h reforming of TD at O/C = 1.2, 0.23 MPa, 900 °C and 50,000 scc $g_{catalyst}^{-1}$ h^{-1}

	0.5 wt% Rh/γ-Al_2O_3	LZ	LRZ	LSRZ
H_2 yield (%)	85	65	83	86
CO yield (%)	79	68	83	89
CO_2 yield (%)	20	21	7	4
CH_4 yield (%)	1	8	5	1
Olefin yield (%)	0.2	3.0	1.0	n.d.[a]
Carbon balance (%)	>99	>99	>96	>95

[a] n.d. – not detected.

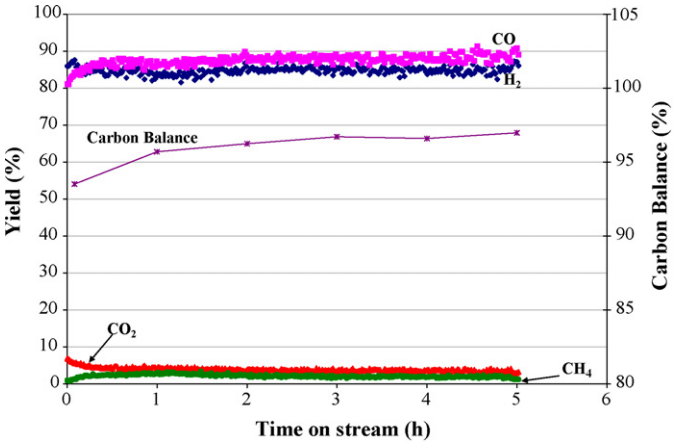

Fig. 4. Carbon balance and yields of yields of H_2, CO, CO_2, and CH_4 during the CPOX of TD over LSRZ for 5 h at an O/C = 1.2, 0.23 MPa, 900 °C and 50,000 scc/$g_{catalyst}$/h. H_2 (♦), CO (■), CO_2 (▲), CH_4 (●), and carbon balance (✻) (For interpretation of the references to colour in this figure legend, the reader is referred to the web version of the article).

produces a noticeably larger quantity of methane, as well as C_2–C_3 hydrocarbons than Rh/γ-Al_2O_3. It is the formation of these products that results in lower H_2 and CO yields and a synthesis gas ratio (H_2/CO) ≤1. A mass balance of hydrogen-containing species in the product stream of LZ shows the equivalent yield of H_2 contained in these hydrocarbons to be between 10 and 11% over the 5 h of the experiment. This indicates that the lower H_2 formation between LZ and Rh/γ-Al_2O_3 can be accounted for by the increase in formation of CH_4, and C_2–C_3 hydrocarbons (mainly ethylene).

The substitution of Rh in LZ and LSZ shows comparable synthesis gas and olefin yields to Rh/γ-Al_2O_3 for the CPOX of TD. This confirms that the available Rh retains its high activity and selectivity after it is substituted into the structure. The activity likely results from the atomically dispersed Rh metal at the surface that are only partially coordinated with oxygen atoms, rather than fully coordinated within the structure. This is consistent with TPR results for LRZ and LSRZ that were presented earlier, in Fig. 3, where a low temperature reduction peak indicates that a small amount of Rh is accessible at the surface and is reducible. In this case, the partial coordination of rhodium permits the metal to readily react with TD (or secondary hydrocarbon products) and oxygen at the surface. A similar behavior was reported by Liu and Krumpelt [35] for the ATR of surrogate diesel fuel mixture using a ruthenium substituted perovskite catalyst. They reported that the most active sites for ATR activity were surface ruthenium atoms distributed at the B-site. The results here also suggest that a catalyst containing only the partially coordinated Rh at the surface of the pyrochlore structure would be active for CPOX. Such a catalyst would avoid the added cost of Rh that is contained within the catalyst, but which does not apparently contribute significantly to the activity. Further, the addition of Sr to the LRZ pyrochlore (forming the LSRZ) improves the activity slightly (Table 5), and significantly reduces methane and olefin yield. The latter is important because olefins are considered the precursors to the formation of carbonaceous

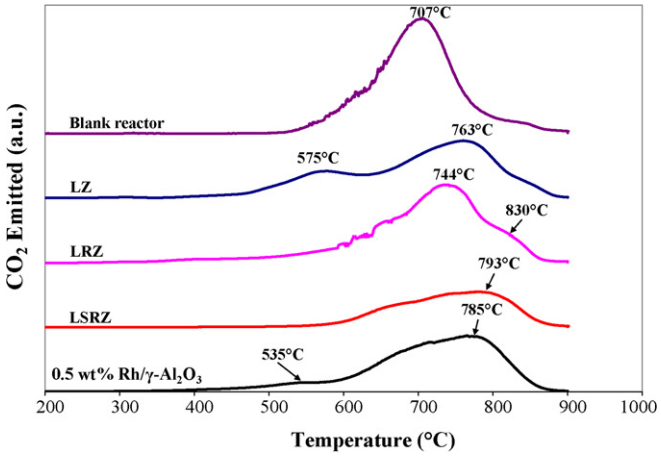

Fig. 5. TPO profiles of carbon deposited on Rh/γ-Al_2O_3, LZ, LRZ, LSRZ, and quartz sand after CPOX of TD.

deposits on the catalyst [5], and their presence suggests that eventual deactivation by carbon is likely.

3.2.3. Carbon formation

As in all hydrocarbon reforming reactions, the CPOX of TD is accompanied by the formation of carbon. Guisnet and Magnoux [63] reported that for hydrocarbon reforming reactions above 350 °C, the adsorbed carbon species generally consist of polyaromatic compounds, which are also known as coke. Therefore, as the CPOX of TD in this study takes place at 900 °C, or higher, it is probable that the carbon formed on each catalyst contains these types of compounds. The carbon/coke content for each catalyst was quantified by a TPO after each 5 h CPOX experiment, and these results are shown in Fig. 5 and Table 6.

The carbon deposited on the surface of the quartz sand is formed as a result of the thermal cracking of TD. Thermal decomposition of TD involves the dehydrogenation of the paraffins into olefins, then the subsequent breakage of C–C bonds into radicals and smaller hydrocarbons [64]. Either of these steps forms reactive products/intermediates that form carbon-containing deposits. These compounds then adsorb on the surface as ordered compounds and require high temperatures for burn-off.

Two peaks arise during the TPO of Rh/γ-Al_2O_3: a small shoulder around 535 °C then a larger peak at 785 °C. These two peaks suggest that carbon has deposited onto different parts of the surface with different reactivities. Several studies have indicated that the low temperature peak can be attributed to the carbon deposited onto the metal, while the high temperature peak can be associated with the more refractory carbon on the support or metal-support interface [21,26,65]. Therefore, the low temperature shoulder, at 535 °C, is probably the carbon deposited on the Rh metal surface. It is oxidized at a lower temperature because the metal catalyzes the oxidation of the carbon. The high temperature peak (observed ~785 °C) is then a result of the carbon deposited on or near the alumina support. This carbon is much more stable, and thus is oxidized at a higher temperature.

Table 6
Carbon deposited after CPOX of TD for 5 h; O/C = 1.2, 0.23 MPa, 900 °C and 50,000 scc $g_{catalyst}^{-1}$ h^{-1}

Catalyst	Carbon accumulated ($g_{carbon}/g_{catalyst}$)
Blank	0.40
LZ	0.29
LRZ	0.32
LSRZ	0.17
Rh/γ-Al_2O_3	0.27

The carbon formed on LZ material is qualitatively and quantitatively similar to the carbon that accumulated on the Rh/γ-Al_2O_3 catalyst. This suggests that there are two parts of the surface that adsorb carbon, and the reactivity of this carbon is similar to that which adsorbs onto the Rh/γ-Al_2O_3. The first peak/shoulder, at roughly 575 °C, may be attributed to a more hydrogenated form of coke, similar to that which adsorbs onto a metallic surface [65]. The high temperature peak may then be due to an unsaturated form of coke [65]. This type of coke would take the form of a dehydrogenated polyaromatic structure, which has a slow oxidation rate and requires a higher temperature for burn-off.

Rhodium substitution alone does not reduce the amount of carbon that accumulates on the pyrochlore material, as the values in Table 6 show that the amount of carbon on LZ and LRZ are relatively the same. However, no low temperature peak is observed for the LRZ that would correspond either to carbon deposited on rhodium metal (seen in the TPO for Rh/Al_2O_3) or reactive coke seen on LZ. The carbon that does accumulate is qualitatively similar to the high temperature carbon on LZ, but there is more of it.

The substitution of lower valence elements into the A-site of oxide catalysts has been shown to create structural defects which lead to the movement of oxygen ions throughout the lattice [35,37,66]. In the presence of a reforming metal, oxygen mobility has been linked to lower carbon formation [35,37]. In the present study, LSRZ has the lowest amount of carbon formed, compared to the other three catalysts studied. This indicates that Sr addition may create structural defects which enhance the oxygen mobility in the material. This in turn, reduces the amount of carbon that is able to form on the surface because carbon deposited on the surface reacts with mobilized oxygen from the lattice to form CO or CO_2. It is unclear, however, whether the oxygen ion movement would be caused by the substitution of Sr into the pyrochlore structure, or a composite effect of the pyrochlore-perovskite phases present. Still, the carbon deposited on LSRZ is qualitatively similar to LRZ, but this catalyst has less carbon (0.17 $g_{carbon}/g_{catalyst}$) than any other catalyst in Table 6 and roughly half that of the non-Sr containing LRZ, (0.32 $g_{carbon}/g_{catalyst}$). Again, there is no TPO peak at 535 °C corresponding to carbon adsorbed on the rhodium, only a TPO peak resembling the high temperature coke on the LZ.

4. Conclusions

Lanthanum zirconate, lanthanum-rhodium-zirconate, and lanthanum-strontium-rhodium-zirconate catalysts were successfully synthesized by a version of the Pechini Method [48]. XRD confirmed the formation of the pyrochlore phase for the LZ and LRZ catalysts. However, the substitution of Sr into the structure (LSRZ) resulted in a defect $SrZrO_3$ perovskite phase

in addition to the cubic pyrochlore phase. Temperature programmed reduction and pulse chemisorption with H_2 showed that the Rh metal was substituted into the pyrochlore structure, with only a small portion of the total metal being reducible.

During the CPOX of *n*-tetradecane, each Rh catalyst produced synthesis gas yields close to equilibrium levels. These high yields for the Rh-substituted pyrochlore catalyst (LRZ and LSRZ) indicate that the Rh metal is able to maintain activity after it is substituted into the structure. The activity of the LRZ and LSRZ is attributed to partially coordinated Rh atoms on the surface. The amount of carbon, or ''coke'' formed on each catalyst after the CPOX of TD was quantitatively similar for each catalyst, with the exception of LSRZ. It was surmised that the substitution of Sr led to oxygen ion mobility in the material which was responsible for the reduction in carbon formation.

Acknowledgements

This work was performed in support of the National Energy Technology Laboratory's on-going research in fuel processing, under contract # DE-AC26-04NT41817 subtask 41817.610.01.01. The authors would also like to gratefully acknowledge Donald Floyd for his invaluable contributions to this work in performing the experiments.

References

[1] S. Ahmed, M. Krumpelt, Int. J. Hydrogen Energy 26 (2001) 291.
[2] D.K. Ross, Vacuum 80 (2006) 1084.
[3] S. Ahmed, R. Kumar, M. Krumpelt, Fuel Cells Bull. 2 (12) (1999) 4.
[4] S. Ahmed, M. Krumpelt, R. Kumar, S.H.D. Lee, J.D. Carter, R. Wilkenhoener, C. Marshall, Fuel Cell Seminar, Palm Springs, CA, 1998.
[5] D. Shekhawat, D.A. Berry, T.H. Gardner, J.J. Spivey, in: J.J. Spivey, K.M. Dooley (Eds.), Catalysis, The Royal Society of Chemistry, Cambridge, 2006, p. 184.
[6] C.-J. Brodrick, T.E. Lipman, M. Farshchi, N.P. Lutsey, H.A. Dwyer, D. Sperling, S.W. Gouse III, D.B. Harris, F.G. King, Trans. Res. Part D: Transport Environ. 7 (2002) 303.
[7] M.C. Williams, J.P. Strakey, W. Sudoval, J. Power Sources 159 (2006) 1241.
[8] M.C. Williams, J.P. Strakey, S.C. Singhal, J. Power Sources 131 (2004) 79.
[9] L. Gaines, National Idling Reduction Conference, Des Moines, IA, 2004.
[10] S. Jain, H.-Y. Chen, J. Schwank, J. Power Sources 160 (2006) 474.
[11] J. Lawrence, M. Boltze, J. Power Sources 154 (2006) 479.
[12] K. Ahmed, K. Foger, Electrochemical Society Proceedings 2003–07, Paris, France, Spring, (2003), p. 1240.
[13] S. Ahmed, R. Kumar, M. Krumpelt, Fuel Cells Bull. 2 (September) (1999) 4.
[14] H.H. Ibrahim, R.O. Idem, Chem. Eng. Sci. 61 (2006) 5912.
[15] A. Lindermeir, S. Kah, S. Kavurucu, M. Muhlner, Appl. Catal. B: Environ. 70 (2007) 488.
[16] Conceptual Design of POX/SOFC 5 kW net System, Final Report, by A.D. Little Inc. U.S. Department of Energy, DDOE/CE/71316-12, 2001.
[17] L.D. Schmidt, E.J. Klein, C.A. Leclerc, J.J. Krummenacher, K.N. West, Chem. Eng. Sci. 58 (2003) 1037.
[18] R.P. O'Connor, E.J. Klein, L.D. Schmidt, Catal. Lett. 70 (2000) 99.
[19] G.J. Panuccio, B.J. Dreyer, L.D. Schmidt, AICHE J. 53 (2007) 187.
[20] G.J. Panuccio, K.A. Williams, L.D. Schmidt, Chem. Eng. Sci. 61 (2006) 4207.
[21] D. Shekhawat, T.H. Gardner, D.A. Berry, M. Salazar, D.J. Haynes, J.J. Spivey, Appl. Catal. A: Gen. 311 (2006) 8.
[22] T.H. Gardner, D. Shekhawat, D.A. Berry, M.W. Smith, M. Salazar, E.L. Kugler, Appl. Catal. A: Gen. 323 (2007) 1.
[23] J.J. Krummenacher, K.N. West, L.D. Schmidt, J. Catal. 215 (2003) 332.
[24] R. Subramanian, G.J. Panuccio, J.J. Krummenacher, I.C. Lee, L.D. Schmidt, Chem. Eng. Sci. 59 (2004) 5501.
[25] J.J. Krummenacher, L.D. Schmidt, J. Catal. 222 (2004) 429.
[26] A. Shamsi, J.P. Baltrus, J.J. Spivey, Appl. Catal. A: Gen. 293 (2005) 145.
[27] K.A. Williams, L.D. Schmidt, Appl. Catal. A: Gen. 299 (2006) 30.
[28] M. Ferrandon, T. Krause, Appl. Catal. A: Gen. 311 (2006) 135.
[29] D.A. Hickman, E.A. Haupfear, L.D. Schmidt, Catal. Lett. 17 (1993) 223.
[30] A. Beretta, P. Forzatti, Chem. Eng. J. 99 (2004) 219.
[31] P.M. Torniainen, X. Chu, L.D. Schmidt, J. Catal. 146 (1994) 1.
[32] J. Barbier, G. Corro, P. Marecot, J.P. Bournonville, J.P. Frank, React. Kinet. Catal. Lett. 28 (1985) 245.
[33] J. Barbier, P. Marecot, J. Catal. 102 (1986) 21.
[34] J. Barbier, in: B. Delmon, G.F. Froment (Eds.), Catalyst Deactivation, Elsevier Science Publilshers, Amsterdam, 1987, p. 1.
[35] D.-J. Liu, M. Krumpelt, Int. J. Appl. Ceram. Technol. 2 (2005) 301.
[36] A. Qi, S. Wang, G. Fu, C. Ni, D. Wu, Appl. Catal. A: Gen. 281 (2005) 233.
[37] P. Erri, P. Dinka, A. Varma, Chem. Eng. Sci. 61 (2006) 5328.
[38] P.J. Wilde, C.R.A. Catlow, Solid State Ionics 112 (1998) 173.
[39] M.A. Subramanian, G. Aravamudan, G.V.S. Rao, Prog. Solid State Chem. 15 (1983) 55.
[40] H. Dai, X. Zhong, J. Li, Y. Zhang, J. Meng, X. Cao, Mater. Sci. Eng., A. 433 (2006) 1.
[41] D. Sedmidubsky, O. Benes, R.J.M. Konings, J. Chem. Thermodyn. 37 (2005) 1098.
[42] H. Zhou, D. Yi, Z. Yu, L. Xiao, J Alloy Compd. 438 (2007) 217.
[43] R. Vassen, X. Cao, F. Tietz, D. Basu, D. Stoever, J. Am. Ceram. Soc. 83 (2000) 2023.
[44] C. Song, C.S. Hsu, I. Mochida, Chemistry of Diesel Fuels, Taylor and Francis, New York, 2000.
[45] F.J. Lepe, J. Fernandez-Urban, L. Mestres, M.L. Martinez-Sarrion, J. Power Sources 151 (2005) 74.
[46] A. Majid, J. Tunney, S. Argue, D. Wang, M. Post, J. Margeson, J. Alloys Compd. 398 (2005) 48.
[47] F. Tietz, A. Schmidt, M. Zahid, J. Solid State Chem. 177 (2004) 745.
[48] M.P. Pechini, Method of preparing lead and alkaline earth titanates and niobates and coating method using the same to form a capacitor, U.S. Patent no. 3330697 (1963).
[49] M. Popa, J. Frantti, M. Kakihana, Solid State Ionics 154–155 (2002) 437.
[50] M.E. Davis, R.J. Davis, Fundamentals of Chemical Reaction Engineering, McGraw-Hill Co., New York, 2003, p. 138 (Chapter 5).
[51] M. Ojeda, M.L. Granados, S. Rojas, P. Terreros, J.L.G. Fierro, J. Mol. Catal. A: Chem. 202 (2003) 179.
[52] K.K. Rao, T. Banu, M. Vithal, G.Y.S.K. Swamy, K.R. Kumar, Mater. Lett. 54 (2002) 205.
[53] I. Hayakawa, H. Kamizono, J. Nucl. Mater. 202 (1993) 163.
[54] S.J. Patwe, A.K. Tyagi, Ceram. Int. 32 (2006) 545.
[55] C.-P. Hwang, C.-T. Yeh, Q. Zhu, Catal. Today 51 (1999) 93.
[56] Z. Li, Y. Fu, M. Jiang, Appl. Catal. A: Gen. 187 (1999) 187.
[57] W.-Z. Weng, X.-Q. Pei, J.-M. Li, C.-R. Luo, Y. Liu, H.-Q. Lin, C.-J. Huang, H.-L. Wan, Catal. Today 117 (2006) 53.
[58] C. Wong, R.W. McCabe, J. Catal. 107 (1987) 535.
[59] A. Roine, HSC Chemistry 4.0 ed., Outokumpu Research Oy, Pori, Finland, 1999.
[60] D.J. Haynes, D.A. Berry, D. Shekhawat, T.H. Gardner, J.J. Spivey, Ind. Eng. Chem. Res., in press.
[61] A. Beretta, E. Ranzi, P. Forzatti, Chem. Eng. Sci. 56 (2001) 779.
[62] N.J. Degenstein, R. Subramanian, L.D. Schmidt, Appl. Catal. A: Gen. 305 (2006) 146.
[63] M. Guisnet, P. Magnoux, Appl. Catal. A: Gen. 212 (2001) 83.
[64] E. Ranzi, M. Dente, A. Goldaniga, G. Bozzano, T. Faravelli, Prog. Energy Combust. Sci. 27 (2001) 99.
[65] J. Barbier, Appl. Catal. A. 23 (1986) 225.
[66] R.M. Navarro, M.C. Alvarez-Galvan, J.A. Villoria, I.D. Gonzalez-Jimenez, F. Rosa, J.L.G. Fierro, Appl. Catal. B: Environ. 73 (2007) 247.